ELSEVIER

Chemical Engineering Journal 120 (2006) 55–61

Chemical Engineering Journal

www.elsevier.com/locate/cej

Textural and fractal properties of CuO/Al_2O_3 catalyst supports

Lj.S. Rožić [a,*], S.P. Petrović [a], T.B. Novaković [a], Ž.D. Čupić [a], Ž.B. Grbavčić [b], D.M. Jovanović [a]

[a] *IChTM, Department of Catalysis and Chemical Engineering, Njegoševa 12, 11000 Belgrade, Serbia and Montenegro*
[b] *Faculty of Technology and Metallurgy, University of Belgrade, Karnegieva 4, 11000 Belgrade, Serbia and Montenegro*

Abstract

Reactive amorphous aluminas with a high surface area, suitable as a precursor for catalyst supports, are obtained by flash calcination of gibbsite in a reactor for pneumatic transport in the dilute two phase flow regime. In the present paper we study the effects of the gibbsite dehydration temperature on the textural and fractal properties of activated aluminas. The parameters of the pore structure for all samples were evaluated from nitrogen adsorption–desorption isotherms. On the basis of the sorption-structure analysis, the fractal dimension of the aluminas surface were determined by three methods, according to Pfeifer and Avnir, Neimark et al. and Mahnke and Mögel, with a goal to compare obtained values. As expected, a good agreement between the results of these methods was achieve. The values of the fractal dimension of activated aluminas increase with the increase of the temperature of thermal treatment, indicating that the irregularities of their surfaces are greater.

Keywords: Pneumatic transport; Flash calcinations; Activated alumina; Fractal dimension

1. Introduction

Supported metal oxide catalysts attract much attention because of their wide application as oxidation catalysts and/or as precursors of the supported metal and sulfide catalysts used in a variety of industrially important reactions. One of the processes very important from the viewpoint of organizing new material technologies is the synthesis of the transition aluminas, as acid–base catalysts like CuO/Al_2O_3, adsorbents for gas and liquids, as well as catalyst carriers. One way of obtaining activated aluminas is thermal treatment of gibbsite, which results in its partial dehydration. Depending on the treatment conditions, products having different properties can be obtained [1–5]. It is already known that the treatment of gibbsite in special regimes, in a reactor for pneumatic transport, i.e. in dilute two-phase flow, makes it possible to obtain amorphous intermediate phases with high surface areas, which are more active than the starting material [3–9]. Due to the latter properties, the activated alumina may be used as a precursor for the preparation of adsorbents and catalysts. The degree of gibbsite amorphization is affected by its physico-chemical properties and thermal treatment conditions (temperature, reaction medium and residence time) [2,5].

The appropriate modeling of the geometry effects can contribute to the improvement of the performance of activated alumina through a rational shape design. Recently, the fractal dimension d_f proved itself to be a useful tool for describing the roughness and irregularities of materials on different scales. There are many different concepts of the fractal dimension depending on how it is determined. From the theoretical point of view, the Hausdorff dimension is the most accurate, but unfortunately for practical purposes it is unsuitable. For surface, many methods were proposed to determine this parameter, some of which made use of adsorption isotherms [10–15]. Fractal dimensions, that describes such fractal materials, were found to be in the range $2 \leq d_f < 3$: low values ($d_f = 2.0$) indicate regularity and smoothness, intermediate d_f values indicate irregular surfaces and d_f values close to 3 indicate highly irregular surfaces. The fractal surfaces are more efficient than planar ones for diffusion limited adsorption processes and therefore, fractal catalytic support has an advantage compared to a non fractal one. The pore-fractal catalysts are particularly interesting since they are sometimes less sensitive and less susceptible to deactivation then planar one. Fractal geometry leads to a minimum in catalyst deactivation [16,17].

2. Experimental

Gibbsite is the best-known crystalline aluminium trihydroxide. It is also the most important aluminium hydroxide, because

* Corresponding author.
E-mail address: srlepp@nanosys.ihtm.bg.ac.yu (Lj.S. Rožić).

1385-8947/$ – see front matter © 2006 Elsevier B.V. All rights reserved.
doi:10.1016/j.cej.2006.03.027

Nomenclature

C	constant, estimated by the Mahnke and Mögel formalism
d	pore diameter (nm)
d_f	fractal dimension
d_p	particle diameter (m)
D_t	diameter of the transport tube (m)
f_p	particle-wall friction coefficient
f_f	fluid-wall friction coefficient
F_f	pressure gradient due to the fluid-wall friction (Pa/m)
F_p	pressure gradient due to the particle-wall friction (Pa/m)
g	gravitational acceleration (m/s^2)
G_f	fluid mass flowrate (kg/s)
G_p	particle mass flowrate (kg/s)
m	number of moles of water eliminated per mol of Al_2O_3 at time t (molH_2O/molAl_2O_3)
m_0	initial number of moles of water per mol of Al_2O_3 (mol H_2O/mol Al_2O_3)
p	measured pressure (Pa)
p_0	vapor pressure of the gas over free fluid surface (Pa)
P	static fluid pressure in transport tube (Pa)
P_r	p/p_0 relative pressure
r_p	pore radius (nm)
Re	pipe Reynolds-number
S_{BET}	specific surface area of materials from B.E.T.-equation (m^2/g)
t	residence time (s)
u	mean interstitial fluid velocity in the transport tube (m/s)
U	superficial fluid velocity (m/s)
u_s	slip velocity between fluid and particles (m/s)
u_{sf}	slip velocity between fluid and particles in a particulately fluidized bed at same voidage as in transport tube (m/s)
U_t	particle terminal velocity in an infinite medium (m/s)
U_{mf}	superficial fluid velocity at minimum fluidization (m/s)
v	particle velocity in the transport tube (m/s)
V	volume of gas adsorbed in cm^3 NTP/g of adsorbent (cm^3/g)
V_m	volume of gas in cm^3 NTP/g of adsorbents that should be able to cover the whole surface with a unimolecular layer ("monolayer capacity") (cm^3/g)
V_p	pore volume (cm^3/g)
z	vertical coordinate (m)

Greek letters

α	3-d_f
β	fluid-particle interphase drag coefficient (kg/m^3 s)
β_{mf}	fluid-particle interphase drag coefficient in a particulately fluidized bed at minimum fluidization (kg/m^3 s)
ε	voidage in the transport tube
ε_{mf}	bed voidage at minimum fluidization
μ	viscosity of the fluid (Pas)
ρ	particle density (kg/m^3)
ρ_f	fluid density (kg/m^3)

it is used as an intermediate for the production of active aluminas. Gibbsite, obtained as the intermediate product in the Bayer process, having a granulation less than10 μm, was used as the starting material. Thermal treatment of gibbsite was performed using the system shown in Fig. 1 [9].

The pilot-scale plant has been designed according to the hydrodynamic model of vertical gas-small particles flow, based on our previous laboratory investigations [3,6]. It consists of a blower for the air supply (1), electric air preheaters (2), a pneumatic transport reactor with a transport tube diameter of 80 mm (3), a mixing chamber for warm and cold air (4), a cyclone (5) and a bag filter (6) for product collection. Gibbsite was introduced into the reaction section using a vibrating feeding device (7) and a pneumatic transport line (8) with an air flow rate of 1 m^3/h. In all runs, the gibbsite flow rate was 2 kg/h. Before starting an experiment, the air was preheated up to the selected reaction temperature adjusted by a temperature inlet controller (TIC). Along the reactor, four thermocouples (TI1–TI4) were situated in the center of the reactor, which ensures the desired temperature profile within the zone of gibbsite decomposition. With a residence time in the heated zone of up to 1 s, gibbsite reaches the chosen temperature from 883 to 943 K. The cold air flow was used to cool the outlet mixture of air and activated gibbsite (4). The characteristics of the gibbsite were as follows: water content 2.79 mol H_2O/mol Al_2O_3, bulk density 2.33 g/cm^3 and S_{BET} 19 m^2/g. The water content of the gibbsite and the obtained products were determined by TG analysis. The X-ray diffraction analysis (XRPD) was performed with a Philips PW 1051 diffractometer, using Cu Kα radiation. The nitrogen adsorption–desorption isotherms of the starting gibbsite and of the activated alumina samples were determined at 77 K, in a high vacuum volumetric apparatus. The samples were previously outgassed at a pressure of 10^{-3} Pa for 4 h, the starting gibbsite at 383 K, and the thermally activated samples at 523 K. The specific surface areas of samples, S_{BET}, were determined by the BET method [18–20] from nitrogen adsorption isotherms up to $p/p_0 = 0.3$. The pore size distribution for all samples was calculated from desorption isotherms branch by the procedure given by Lippens et al. [19]. The fractal dimension of the surfaces, d_f, for the starting gibbsite and the activated alumina samples, was calculated by introducing the pore size distribution data into the Pfeifer and Avnir relation [11–13]. According to the Mahnke and Mögel method based on an approximation of the fractal version of the BET-formula the fractal dimensions, d_f, were calculated

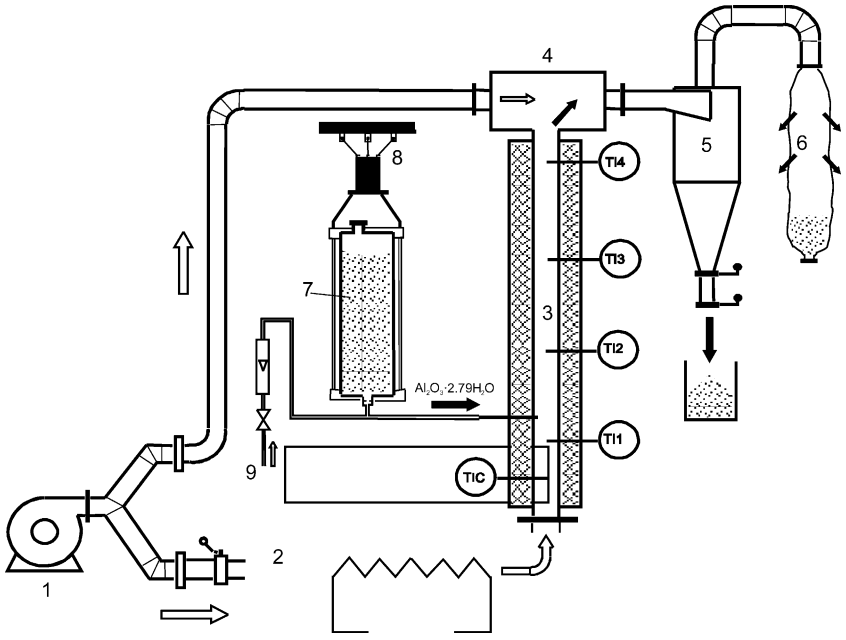

Fig. 1. Schematic diagram of the pilot-scale reactor.

for all samples [14]. For comparison, the method of Neimark et al. was applied to the same isotherms [15].

3. Results and discussion

The assumption for both the preliminary laboratory investigations and the design of the pilot-scale plant was that the gibbsite particles have the same linear velocity as the gas in the reactor. In order to verify this assumption, calculations using a model for two phase flow were performed. This model is described in detail in our previous paper [6]. The bases of the model are the continuity and momentum equations of Nakamura and Capes [21] and Grbavčić [22] variational model for calculating the fluid-particle interphase drag coefficient.

A summary of the relevant model equations for the fluid and particle phases are:

Fluid momentum:

$$\varepsilon\left(-\frac{\mathrm{d}P}{\mathrm{d}z}\right) = \beta(u-v) + \varepsilon\rho_\mathrm{f} g + F_\mathrm{f} \tag{1}$$

Solids momentum:

$$(1-\varepsilon)\left(-\frac{\mathrm{d}P}{\mathrm{d}z}\right) = -\beta(u-v) + (1-\varepsilon)\rho_\mathrm{p} g + F_\mathrm{p} \tag{2}$$

The pressure gradient in the tube is given by the sum of Eqs. (1) and (2) as:

$$-\frac{\mathrm{d}P}{\mathrm{d}z} = (\rho_\mathrm{p}-\rho_\mathrm{f})g(1-\varepsilon) + F_\mathrm{f} + F_\mathrm{p} \tag{3}$$

F_f and F_p are pressure losses due to the fluid-wall and particle-wall friction written in terms of the friction factors f_f and f_p:

$$F_\mathrm{f} = \frac{2 f_\mathrm{f}\rho_\mathrm{f} U^2}{D_\mathrm{t}} \tag{4}$$

$$F_\mathrm{p} = \frac{2 f_\mathrm{p}\rho_\mathrm{p}(1-\varepsilon)v^2}{D_\mathrm{t}} \tag{5}$$

The resulting equation for the slip velocity in a one-dimensional steady state model of vertical non-accelerating gas-fine particles flow is:

$$u_\mathrm{s} = (u-v) = u_\mathrm{sf} F^* \tag{6}$$

where u_sf is the slip velocity in particulately fluidized bed at the same voidage:

$$u_\mathrm{sf} = \frac{(\rho_\mathrm{p}-\rho_\mathrm{f})g(1-\varepsilon_\mathrm{mf})}{\left(\frac{\beta_\mathrm{mf}}{\varepsilon_\mathrm{mf}}\right)} \tag{7}$$

where

$$\beta_\mathrm{mf} = \frac{\varepsilon_\mathrm{mf}(\rho_\mathrm{p}-\rho_\mathrm{f})g(1-\varepsilon_\mathrm{mf})}{\frac{\beta_\mathrm{mf}}{\varepsilon_\mathrm{mf}}} \tag{8}$$

The dimensionless fluid-particle interphase drag coefficient (β) is determined by a variation model [21]

$$\beta = \beta_\mathrm{mf}\left\{1 - C_2 + \frac{1}{\lambda}\left[1 - \left(\lambda\frac{\varepsilon-\varepsilon_\mathrm{mf}}{1-\varepsilon_\mathrm{mf}} + C_1\right)^2\right]^{0.5}\right\} \tag{9}$$

The constants C_1, C_2 and λ are

$$C_1 = \left[1 + \left(\frac{U_\mathrm{mf}^2}{\varepsilon_\mathrm{mf}^3 U_\mathrm{t}^2}\right)^2\right]^{-0.5} \tag{10}$$

$$C_2 = \frac{1}{\lambda}(1-C_1^2)^{0.5} \tag{11}$$

$$\lambda = \left(1-C_1^2\right)^{0.5} - C_1 \tag{12}$$

F^* is the dimensionless friction factor, which is determined by Eq. (13)

$$F^* = 1 + \frac{F_p}{(\rho_p - \rho_f)g(1-\varepsilon)} - \frac{(1-\varepsilon)}{\varepsilon}\frac{F_f}{(\rho_p - \rho_f)g(1-\varepsilon)} \quad (13)$$

The fluid friction coefficient for smooth transport tubes can be accurately predicted using the standard friction factor correlation:

$$f_f = \frac{0.0791}{Re^{0.25}} \quad (14)$$

where the tube Reynolds number is based on the superficial gas velocity ($Re = D_t\rho_f U/\mu$).

Above set of equations can be solved numerically in order to predict particle velocity and voidage in the reaction section. On such way residence time of gibbsite particles in the reaction zone can be adjusted according to the process requirements. The model gives predictions for the transport line voids and the particle phase velocity, for particles smaller than 1 mm, using the experimental values of the gas velocity and the overall pressure gradient. The results show that the gas phase velocity and the particle phase velocity are nearly the same and that the transport line voids are higher than 0.99. Therefore, under the conditions applied in our experiments, there is dilute two phase flow, and the particle residence time in the reaction section can be calculated on the basis of measured gas phase velocity. In the course of the thermal activation of gibbsite under the chosen experimental conditions, flash calcination of the gibbsite into products with a smaller amount of water occurs, depending on the time spent in the degradation zone and the activation temperature. The dependence of the crystalline water content on the residence time at four chosen temperatures is shown in Table 1.

The experimental results show that under the selected conditions of temperature and residence time in the heated zone, the gibbsite is partially dehydrated. As expected, the degree of dehydration increases with increasing the activation temperature. At the same dehydration temperature, the degree of dehydration increases with increasing the particle residence time. The linear dependence between $\ln(m_0-m)$ and the residence time indicates that the dehydration reaction follows first-order kinetics. We evaluated the rate constants (k) from the slope of these curves and used them to calculate the activation energy of gibbsite dehydration in the temperature range of 883–943 K, from the Arrhenius equation. The value of the activation energy is equal to 66.5 kJ/mol [9].

Table 1
Water content (m_0-m) mol H_2O/mol Al_2O_3 in products obtained on thermal treatment of gibbsite

t (s)	$(m_0-m)_{883\,K}$	$(m_0-m)_{903\,K}$	$(m_0-m)_{923\,K}$	$(m_0-m)_{943\,K}$
0.00	2.79	2.79	2.79	2.79
0.38	1.99	1.69	1.60	1.24
0.58	1.60	1.51	1.00	1.00
0.65	1.42	1.16	0.92	0.77
0.73	1.24	1.08	0.92	0.77
0.81	1.24	1.16	0.77	0.63

The experimental results show that the products having water content similar to the stoichiometric water content for alumina monohydrate were obtained at all measured temperatures for a residence time of 0.73 s. A short residence time of the pseudofluidized gibbsite particles in the zone of high temperatures prevents the crystallization of the material into new phases. Gibbsite is denoted as MPA0, and the activated samples as MPA1, MPA2, MPA3, MPA4, respectively with an increase of the dehydration temperatures.

The X-ray diffraction (XRPD) can give valuable information about the morphology and the surface structure. The XRPD for gibbsite and activated alumina samples are presented in Fig. 2.

In analyzing the XRPD data, the pure crystal gibbsite phase was identified for the starting samples. A decrease in the reflection intensity of gibbsite with increasing temperature indicates that the activated aluminas are either microcrystalline or amorphous.

The complete nitrogen adsorption–desorption isotherms of the gibbsite and of the activated alumina samples are shown in Fig. 3.

All isotherms at low equilibrium pressures are reversible, whereas at higher equilibrium pressures they exhibit a hysteresis loop of the H3 type [20]. This type of hysteresis loop indicates the presence of slit-shaped mezopores or pores with narrow necks and wide bodies in the activated aluminas. All adsorption isotherm near to $p/p_0 = 1$ are very steep, which is characteristic for the presence of macropores between aggregates. The values of the specific surface areas, S_{BET}, of gibbsite and the activated alumina samples, calculated from these isotherms, are given in Table 2. As can be seen, upon thermal activation in a temperature range from 883 to 943 K, rapidly evaporated water from

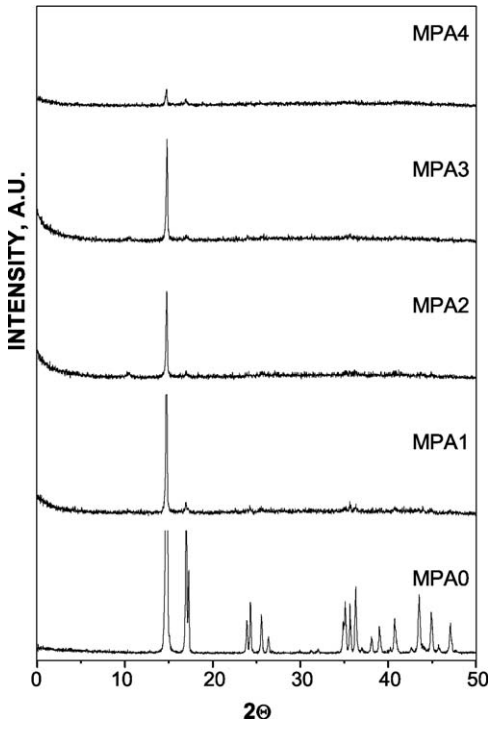

Fig. 2. XRPD of the gibbsite and activated alumina samples.

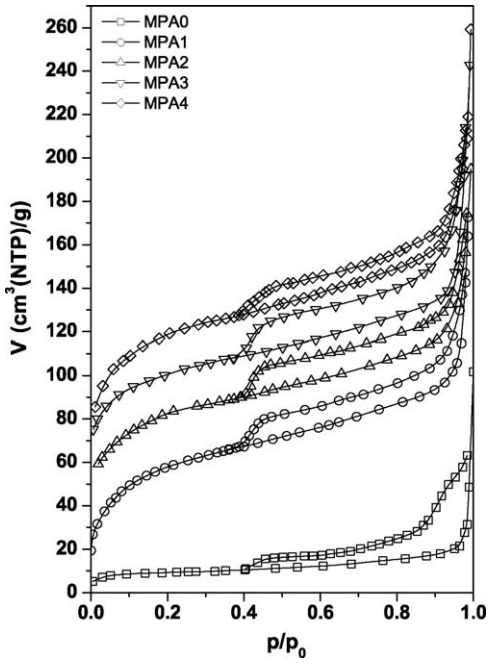

Fig. 3. Nitrogen adsorption isotherms of gibbsite and activated alumina samples. The ordinate scales are moved up by 20 cm^3 (NTP)/g for successive results from MPA1 to MPA4.

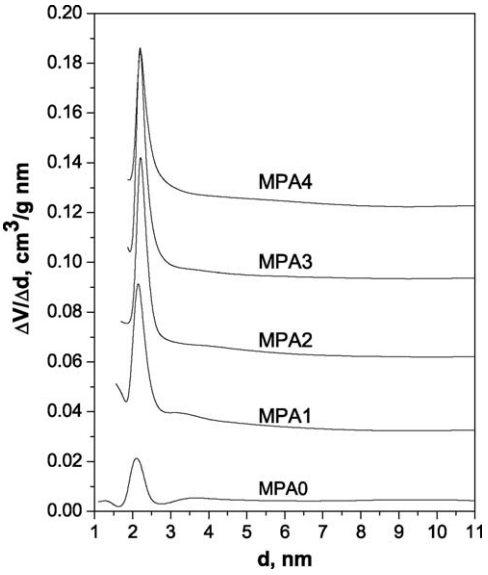

Fig. 4. Derivative of the cumulative pore volume curves with respect to slit width for gibbsite and activated alumina samples. The ordinate scales are moved up by 0.03 cm^3/g nm for successive results from MPA1 to MPA4.

gibbsite comes under a great pressure from inside of the grains to the surface, causing an increase of the specific surface area up to 250 m^2/g.

The data derived from the cumulative pore volume curves of the gibbsite and the activated alumina samples (Fig. 4) show that the starting gibbsite, within the investigated region of micro- and mezopores, is characterized by a wide pore size distribution, the pore diameter of 2–2.5 nm being the most frequent. All of the activated alumina samples have most of the pores with a diameter of 2–2.5 nm, similar to the starting gibbsite, but the pore volumes within this range increase from 0.165 to 0.320 cm^3/g, with increasing the treatment temperature from 883 to 943 K. The data also indicates that the activated alumina samples possess micropores whose volume increases with the temperature of the thermal treatment, within the whole investigated temperature range.

Introducing the pore size distribution data into the Pfeifer and Avnir relation [11] which relates the pore size distribution with the fractal dimension of the surface, d_f:

$$-\left(\frac{dV_p}{dr_p}\right) \propto r_p^{(2-d_f)} \tag{15}$$

Table 2
Fractal dimension values calculated using different methods

Sample	Method			S_{BET} (m^2/g)
	Pfeifer and Avnir	Mahnke and Mögel	Neimark	
MPA0	2.02	–	2.14	19
MPA1	2.29	2.24	2.22	199
MPA2	2.31	2.38	2.27	215
MPA3	2.38	2.40	2.35	220
MPA4	2.40	2.44	2.39	251

the fractal dimensions of the surface, d_f, for the starting gibbsite and for the activated alumina samples were calculated. The estimation of d_f values was performed in the region of small pores, $0.5 < r_p < 2$ nm. The logarithmic form of Eq. (15) was used. From the slope of this linear relationship the fractal dimension was computed for all of the samples (Table 2).

Another approach uses the extended BET-formalism for the fractal-like surfaces [10]. Mahnke and Mögel [14] suggested an alternative derivation of a fractal BET equation to that initially proposed by Fripiat et al. The alternate derivation avoids the inconsistent behavior, of the earlier equation, in the case of a surface fractal dimension of 3. The isotherm equation derived by Mahnke and Mögel [14] is given by

$$\log(V(P_r)) = \log(V_m) + \log\frac{CP_r}{1 - P_r + CP_r} - \alpha\log(1 - P_r) \tag{16}$$

This logarithmic version of the equation of Mahnke and Mögel (2) gives the possibility to estimate the optimal (with respect to mean square error) α, C and V_m for measured isotherms using the simplex optimization method [23]. The obtained values of the fractal dimension of the surfaces for all the samples are given in Table 2.

For comparison, the method of Neimark [15] is applied to the same isotherms. The fractal assumption is made for the interface area of the adsorbate depending on the radius of curvature. They presented the equation

$$\log\left(-\int_{V(p)}^{V_{max}} \log(P_r)dV\right) = \text{const} + (d-2)\log(-\log P_r) \tag{17}$$

where the integral was taken to be $\int_{V(p)}^{V_{max}} \log(V^{-1}(x))dx$ and evaluated using trapezoidal rule, and x is relative pressure.

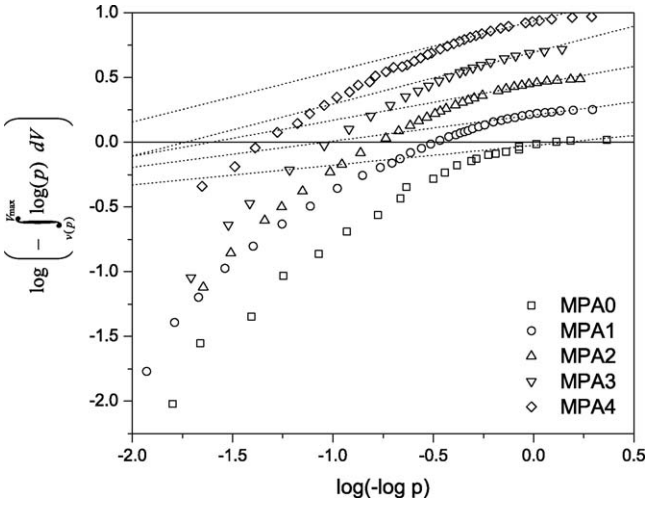

Fig. 5. Estimation of fractal dimension according to Neimark's method. The ordinate scales are moved up by 0.25 for successive results from MPA1 to MPA4.

From the slopes of the corresponding plots (Fig. 5) the fractal dimensions for all of the samples are calculated and shown in Table 2.

The fractal dimension of the gibbsite (MPA0) is near 2, which indicates that the size of the irregularities of its surface is larger than the size of the adsorbate. It should be mentioned that we were not able to perform a satisfying calculation of d_f for the MPA0 sample using Mahnke and Mögel method.

In spite of the small differences between the values of the fractal dimension for the activated alumina samples, all of them show the same trend of the changes in the fractal dimension. The increase of the values of the fractal dimension of the activated aluminas with the thermal treatment temperature indicates the roughness enhancement of their surfaces.

Therefore, all of the three methods used for the evaluation of the fractal dimension gives, roughly speaking, a correct result. From the practical point of view, the methods of Mahnke and Mögel, and Neimark are much easier to apply because these are free from many of the complications in the original method developed by Avnir and co-workers.

According to some authors [16,17] the pore-fractal catalysts supports are superior to the planar ones in the case of diffusion limited reactions and catalyst deactivation. The proposed treatment of the gibbsite in the reactor for the pneumatic transport is suitable for the preparation of catalyst supports with fractal pore-structure.

In our future work we try to correlate the change of fractal pore structure of the catalyst support with the changes of the properties of catalysts during deactivation.

4. Conclusion

Upon the thermal activation of gibbsite in a reactor for pneumatic transport, i.e. in dilute two-phase flow with the short particle residence time of 0.73 s in a homogenous temperature zone, intermediate pseudoamorfous aluminas were obtained with a developed porosity in region of micro- and mezopores. The specific surface areas of the activated alumina samples ranged from 199 to 251 m^2/g, depending on the temperature of their formation.

The fractal dimensions of the surface of gibbsite and the activated alumina samples were calculated by applying three different methods. It was shown that the values of fractal dimensions increase from 2.02 to 2.45 with the increasing temperature of gibbsite activation, pointing to changes in the texture of the alumina surface. As already mentioned, from the practical point of view, the methods of Mahnke and Mögel, and Neimark are much easier for the application than the original method developed by Avnir and co-workers.

The reactor for the pneumatic transport is suitable for the preparation of catalyst supports with fractal pore-structure.

Acknowledgements

This work was supported by the Ministry of Science and Environmental Protection of the Republic of Serbia (Projects number TR 6712B and ON 142019).

References

[1] B.C. Lippens, J.H. de Boer, Study of phase transformations during calcination of aluminium hydroxides by selected area electron diffraction, Acta Cryst. 17 (1964) 1312.
[2] S. Engels, U. Bollmann, J. Kobelke, R. Lange, K. Becker, P. Kraak, Highly reactive aluminas as catalyst precursors-a new approach to preparation, heterogeneous catalysis, in: Proceedings of the 6th International Symposium of Heterogeneous Catalysis, Pub. House Bulgar, Academy of Sciences, Sofia, Part 2, 1987, p. 351.
[3] N. Jovanović, T. Novaković, J. Janaćković, A. Terlecki-Baričević, Properties of activated alumina obtained by flash calcination of gibbsite, J. Colloid Interface Sci. 150 (1992) 36.
[4] V.A. Dzisko, Osnovy metodov prigotovleniya katalizatorov, Nauka-Sib, Otdel, Novosibirsk, 1983.
[5] P.A. Buyanov, O.P. Krivoruchko, B.P. Zolotovskii, O prirode termokhimicheskoi aktivacii kristalicheskikh gidroksidov, Izv. Acad. Nauk SSSR Ser. Khim 11 (1986) 39.
[6] Ž. Grbavčić, Lj. Rožić, R. Garić-Grulović, Hydrodynamic model of two-phase flow of gas-small particles, Procesna tehnika 1 (1997) 23.
[7] Lj. Rožić, R. Garić-Grulović, T. Novaković, Ž. Grbavčić, Possibylities of flash calcination of gibbsite in the reactor for pneumatic transport, Forth International Conference on Fundamental and Applied Aspects of Physical Chemistry Papers, Beograd, 1998 p. 422.
[8] Lj. Rožić, R. Garić-Grulović, Ž. Grbavčić, Hydrodynamic modeling of vertical gas-sand particles flow, Thirteenth International Congress of Chemical and Process Engineering, Praha Czech Republic, 1998.
[9] Lj. Rožić, T. Novaković, N. Jovanović, A. Terlecki-Baričević, Ž. Grbavčić, The kinetics of the partial dehydration of gibbsite to activated alumina in a reactor for pneumatic transport, J. Serb. Chem. Soc. 66 (4) (2001) 273.
[10] J.J. Fripiat, L. Gatineau, H. Van Damme, Multilayer physical adsorption on fractal surfaces, Langmuir 2 (1986) 562.
[11] P. Pfeifer, D. Avnir, Chemistry in noninteger dimensions between two and three, I. Fractal theory of heterogeneous surfaces, J. Chem. Phys. 79 (1983) 3558.
[12] D. Avnir, D. Farin, Chemistry in noninteger dimensions between two and three. II. Fractal surfaces of adsorbents, J. Chem. Phys. 79 (1983) 3566.
[13] D. Farin, D. Avnir, The Fractal Approach to Heterogeneous Chemistry, Wiley, 1990, 271.

[14] M. Mahne, H.J. Mögel, Fractal analysis of physical adsorption on material surfaces, Colloids Surf. A: Physicochem. Eng. Aspects 216 (2003) 215.
[15] A.V. Neimark, Determination of surface fractal dimensions from experimental adsorption data, Russ. J. Phys. Chem. (Transl. Zh. Fiz. Khim.) 64 (1990) 1397.
[16] P. Mougin, M. Pons, J. Villermaux, Reaction and diffusion at an artificial fractal interface: evidence for a new diffusional regime, Chem. Eng. Sci. 51 (10) (1996) 2293–2302.
[17] M. Sheintuch, Reaction engineering principles of processes catalyzed by fractal solids, Catal. Rev. 43 (3) (2001) 233–289.
[18] S.H. Gregg, K.S. Sing, Adsorption, Surface Area and Porosity, Academic Press, New York, 1967.
[19] B.C. Lippens, B.G. Linsen, J.H. de Boer, Studies on pore system in catalysts I. The adsorption of nitrogen; apparatus and calculation, J. Catal. 3 (1964) 32.
[20] K. Sing, D. Everet, R. Haul, L. Moscou, R. Pierotti, J. Rouquerol, T. Siemieniewska, Reporting physisorption data for gas/solid systems with special reference to the determination of surface area and porosity, Pure Appl. Chem. 57 (1985) 603.
[21] K. Nakamura, C.E. Capes, Vertical pneumatic conveying: a theoretical study of uniform and annular particle flow models, Can. J. Chem. Eng. 51 (1973) 39.
[22] Ž.B. Grbavčić, R.V. Garić, Dž.E. Hadžismajlović, S.Dj. Jovanović, D.V. Vuković, H. Littman, M.H. Morgan III., Variational model for prediction of the fluid-particle interphase drag coefficient and particulate expansion of fluidized and sedimentings beds, Powder Technol. 68 (1991) 199.
[23] J.A. Nelder, R. Mead, A simplex method for function minimization, Comput. J. 7 (1965) 308.